Arabian Journal of Chemistry (2020) 13, 9216–9230

King Saud University

Arabian Journal of Chemistry

www.ksu.edu.sa
www.sciencedirect.com

ORIGINAL ARTICLE

Phytochemical and Biological Characterization of *Tephrosia nubica* Boiss. Growing in Saudi Arabia

Hanan M. Al-Yousef [a], Sahar Abdelaziz [b,*], Wafaa H.B. Hassan [b], May A. El-Sayed [b]

[a] *Department of Pharmacognosy, College of Pharmacy, King Saud University, Riyadh, Saudi Arabia*
[b] *Department of Pharmacognosy, Faculty of Pharmacy, Zagazig University, 44519 Zagazig, Egypt*

Received 3 September 2020; accepted 1 November 2020
Available online 11 November 2020

KEYWORDS

Tephrosia nubica;
UPLC-ESI-MS/MS;
Antioxidant;
Cytotoxicity;
Anti-obesity

Abstract The chloroform (TNC), ethyl acetate (TNE) and *n*-butanol (TNB) fractions of *Tephrosia nubica* Bioss. growing in Saudi Arabia were investigated for the first time using UPLC-ESI-MS/MS in two ionization modes. The analysis revealed the tentative identification of 107 compounds. Moreover, the therapeutic potential of *T. nubica* fractions was determined by *in vitro* evaluation of their cytotoxic, antioxidant, and anti-obesity activities using MTT assay, DPPH radical scavenging activity and pancreatic lipase inhibitory assay, respectively. The results showed that TNE, TNB, TNC fractions revealed weak antioxidant activity with SC_{50} 139.9 ± 0.8, 144.9 ± 1.5, 148.9 ± 1.3 μg/mL, respectively compared to ascorbic acid 14.2 ± 0.5 μg/ml. Moreover TNE, TNC fractions showed more significant cytotoxic activity against HepG-2 with IC_{50} 82.1 ± 3.1, 101 ± 2.8 μg/mL and MCF-7 with IC_{50} 114 ± 3.2, 124 ± 3.9 μg/mL respectively. The TNB fraction showed weak cytotoxic activity against both cell lines compared to the other fractions. Ultimately, TNE fraction showed a remarkable anti-obesity activity with IC_{50} 62.4 ± 1.5 μg/mL compared to chloroform fraction with IC_{50} 535.6 ± 2.1 μg/mL and *n*-butanol fraction which did not show any activity. In conclusion, these findings represent the first insights into the phytochemical constituents and pharmacological properties of *T. nubica*. The ethyl acetate fraction of *T. nubica* might be a promising source of functional constituents with antioxidant, cytotoxic and anti-obesity potentials. It might be a natural alternative therapy and nutritional strategy, for obesity treatment without dangerous side effects. Isolation of the bioactive compounds from the ethyl acetate fraction of *T. nubica* and evaluating their biological activities are recommended.

1. Introduction

Genus *Tephrosia* belongs to the family Fabaceae (Papilionaceae). This genus includes around 400 species eight of them are present in Saudi Arabia. Plants of this genus are annual perennial, prostrate or erect herbs or woody shrubs widely distributed in tropical and sub-tropical regions all over the world (Al-Ghamdi 2013; Touqeer et al. 2013). Many of

* Corresponding author.
E-mail address: Sah_abdelaziz38@yahoo.de (S. Abdelaziz).
Peer review under responsibility of King Saud University.

Production and hosting by Elsevier

https://doi.org/10.1016/j.arabjc.2020.11.006
1878-5352

Tephrosia plants have valuable traditional uses for the treatment of different diseases such as respiratory disorders, rheumatic pains, syphilis, dropsy, diarrhea, asthma, stomach ache, inflammation and wound healing. Additionally, most of *Tephrosia* species are characterized by the presence of variable constituents with anti-cancer, antioxidant, larvicidal and antiviral activities (Martinez et al. 2012; Touqeer et al. 2013). Variable classes of compounds are reported in the plants of this genus like chalcones, rotenoids, glucosides, terpenoids, sterols, essential and fixed oils, with the abundance of flavonoids such as flavanols, flavanones, prenylated flavonoids and isoflavones (Chen et al. 2014; Touqeer et al. 2013; Lodhi et al. 2013).

Isoflavones are found predominantly in most of the Fabaceae plants. They have exceptionally amazing therapeutic characteristics. In addition to the antimycotic, anti-inflammatory, and radical scavenging properties, isoflavones considered as phytoestrogens as they show estrogenic and antiestrogenic activities. They have been associated with a decreased risk of arthritis, hormone dependent cancers and neurodegenerative disorders. They also decrease the risk of diseases result from hormonal deficiency such as osteoporosis and cardiovascular troubles after menopause. Isoflavons may be important antioxidant agents since they exhibit hydroxyl groups in rings A and/or B and are thus, capable of donating hydrogen to free radicals (Hanganu et al. 2010).

T. nubica includes two subspecies, ssp. nubica and ssp. arabica (Boiss) which are present on the west costal region of Saudi Arabia. Up till now there are no reports on the phytoconstituents or the biological activities of *T. nubica* growing in Saudi Arabia. Therefore, it was deemed of interest to investigate the chemical composition of *T. nubica* chloroform, ethyl acetate and *n*-butanol fractions to identify their bioactive compounds using UPLC-ESI-MS/MS analysis in addition to the estimation of their antioxidant, cytotoxic and anti-obesity activities. Further studies are planned to isolate and identify major compounds from the most active fraction using variable spectroscopic and spectrometric techniques for future *in vivo* biological investigation.

2. Materials and methods

2.1. Plant material

The aerial parts of *T. nubica* Bioss. Fabaceae (Papilionaceae), were collected from south region of Saudi Arabia (20°0′0′' N 42°36′0′' E/ 20.00000°N 42.60000°E) in Feb 2014. Plant material was identified by Prof. Dr. Mohamed Yousef from the Pharmacognosy Department, College of Pharmacy, King Saud University and a Voucher specimen (TN/ 16244/14) was deposited in the herbarium of the Pharmacognosy Department, College of Pharmacy, King Saud University, Saudi Arabia.

2.2. Preparation of T. Nubica crude hydroalcoholic extract and fractions

Ethanol 95% (3x 3L) was used for the extraction of the air dried powdered aerial parts of *T. nubica* (1000 g). The dried hydroalcoholic extract (249.0 g) was diluted with water/ methanol (1: 9) mixture and then successively partitioned with *n*-hexane, chloroform, ethyl acetate, and *n*-butanol to give 45.0 g, 38.4 g, 26.0 g, 36. 2 g of *n*-hexane, chloroform (TNC), ethyl acetate (TNE) and *n*-butanol (TNB) fractions respectively.

2.3. UPLC- ESI- MS/MS instrument and separation technique

Ultra performance liquid chromatography with electrospray ionization quadrupole linear ion trap tandem mass spectrometry analysis performed on ESI-MS positive and negative ion acquisition modes was carried out on a XEVO TQD triple quadruple instrument. Method in a multiple-reaction monitoring (MRM) mode was employed for the quantitative determination of phytochemicals. TNC, TNE and TNB fractions were analyzed by UPLC, in order to obtain chromatographic profiles of the more polar portions of the extracts, which contain phenolic and flavonoid compounds. The samples were dissolved in HPLC grade methanol, filtered through 0.2 µm membrane disc filter and resulting solution concentrations were in 0.2 to 0.5 mg/mL range, depending on each fraction. The UPLC system was a Waters Corporation, Milford, MA01757 U.S.A, mass spectrometer. The reverse-phase separations were performed (ACQUITY UPLC - BEH C 18 1.7 µm − 2.1 × 50 mm Column. (50 mm × 1.2 mm [inner diameter] and 1.7 µm particle size) at 0.2 m/mL flow rate. A previously reported gradient program was applied for the analysis (Hassan et al., 2019). The mobile phase comprised of acidified water containing 0.1% formic acid (A) and acidified methanol containing 0.1% formic acid (B). The employed elution conditions were: 0–2 min 10% B isocratic; 2–5 min, linear gradient B 10 to 30%; 5–15 min, linear gradient from 30% to 70% B; 15–22 min, linear gradient from 70% to 90% B; 22–25 min, 90% B isocratic and finally washing and reconditioning of column was done. Electrospray ionization (ESI) was performed in both negative and positive ion modes to obtain more data. The parameters for analysis were carried out using negative ion mode as follows: source temperature 150 °C, cone voltage 30 eV, capillary voltage 3 kV, desolvation temperature 440 °C, cone gas flow 50 L/h, and desolvation gas flow 900 L/h. Mass spectra were detected in the ESI between m/z 100–1000 atomic mass unit. Chemical constituents were identified by their ESI- QqQLIT–MS/MS spectra and fragmentation patterns. The peaks and spectra were processed using the Maslynx 4.1 software and tentatively identified by comparing its retention time (R_t), mass spectrum with reported data and Library search (such as FooDB (http://www.Foodb.ca)).

2.4. Antioxidant assay

The antioxidant activity of TNC, TNE and TNB fractions of *T. nubica* Boiss was determined at the Regional Center for Mycology and Biotechnology (RCMB) at Al-Azhar University, Cairo, Egypt, using the free radical 2,2-diphyenylpicrylhydrazyl (DPPH) scavenging assay, as described by (Al Khateeb et al. 2017).

2.4.1. DPPH radical scavenging activity (Yen and Duh 1994)

Freshly prepared (0.1 mM) solution of 2,2-diphenyl-1-picrylhydrazyl (DPPH) and different tested extracts prepared at 5, 10, 20, 40, 80, 160 and 320 µg/mL in methanol were used and stored at 10 C° in the dark (Gülçin et al. 2004). Absorbance measurements of the DPPH radical without antioxidant

(control) and the reference compound ascorbic acid (5, 10, 20, 40, 80, 160 and 320 μg/mL) were recorded immediately with a UV–visible spectrophotometer (Milton Roy, Spectronic 1201). All the determinations were performed in three replicates and averaged. The percentage inhibition of the DPPH radical was calculated according to the formula:

$$\%\ \text{DPPH radical - scavenging} = [\{(AC - AS)/AC\}\ \mathbf{x\ 100}]$$

where AC = Absorbance of the control solution and AS = absorbance of the sample in DPPH solution.

The percentage of DPPH radical-scavenging was plotted against each extract concentrations and ascorbic acid (μg/mL) to determine scavenging capacity (SC_{50}) which is the concentration required to scavenge DPPH by 50% (i.e. concentration giving 50% reduction in the absorbance of a DPPH solution from its initial absorbance).

2.5. Cytotoxicity assay

The cytotoxic effect of *T. nubica* fractions (TNC, TNE, TNB) against HepG-2 and MCF-7 cells was investigated using 3-(4, 5- dimethylthiazole-2-yl)-2, 5- diphenyl-tetrazolium bromide (MTT) against DMSO and cisplatin as negative and positive controls, respectively. HepG-2 and MCF-7cell lines were obtained from American Type Culture Collection (ATCC, Rockville, MD). The cells were propagated on Dulbecco's modified Eagle's medium (DMEM) supplemented with 10% heat-inactivated fetal bovine serum, 1% L-glutamine, HEPES buffer and 50 μg/mL gentamycin. The cells were maintained at 37 °C in a humidified atmosphere with 5% CO_2 and were subcultured two to three times a week. For antitumor assays, the tumor cell lines were suspended in medium at concentration $5x10^4$ cell/well in Corning® 96-well tissue culture plates, and then incubated for 24 hr. The tested extracts were then added into 96-well plates (six replicates) to achieve eight concentrations for each extract. Six vehicle controls with media or 0.5% DMSO were run for each 96 well plate as a control. After incubating for 24 h, the numbers of viable cells were determined by the MTT test. Briefly, the media was removed from the 96 well plates and replaced with 100 μL of fresh culture DMEM medium without phenol red then 10 μL of the 12 mM MTT stock solution (5 mg of MTT in 1 mL of phosphate buffered saline (PBS)) to each well including the untreated controls. The 96 well plates were then incubated at 37 °C and 5% CO_2 for 4 h. An 85 μL aliquot of the media was removed from the wells, and 50 μL of DMSO was added to each well and mixed thoroughly with the pipette and incubated at 37 °C for 10 min. Then, the optical density was measured at 590 nm with the microplate reader (SunRise, TECAN, Inc, USA) to determine the number of viable cells and the percentage of viability was calculated.

Cell viability % = $[1\text{-}(OD_t/OD_c)]x100\%$ where,

OD_t is the mean optical density of wells treated with the tested sample and ODc is the mean optical density of untreated cells.

The relation between surviving cells and each extract concentration (1–500 μg/mL) is plotted to get the survival curve of each tumor cell line after treatment with the tested fraction. The 50% inhibitory concentration (IC_{50}), the concentration required to cause toxic effects in 50% of intact cells, was estimated from graphic plots of the dose response curve (log extract concentration on X-axis vs. percentage viability from untreated cells on Y-axis) for each conc. using non-linear regression analysis (Dose-response inhibition, log inhibitor vs. normalized response-variable slop) of GraphPad Prism 5 software (GraphPad Software, San Diego, California) (Gomha et al. 2015; Mosmann 1983). All experiments were repeated at least three times. Results are reported as means ± SD.

2.6. In vitro anti-obesity activity using pancreatic lipase inhibitory assay

The lipase inhibition activity of TNC, TNE and TNB fractions of *T. nubica* was determined by (Kim et al. 2010) method. In this assay, the porcine pancreatic lipase activity was measured using *p*-nitrophenyl butyrate (NPB) as a substrate. Lipase solution (100 μg/mL) was prepared in a 0.1 mM potassium phosphate buffer (pH 6.0). Samples with different concentrations (7.81–1000 μg/mL) were pre-incubated with 100 μg/mL of lipase for 10 min at 37 °C. The reaction was then started by adding 0.1 mL NPB substrate. After incubation at 37 °C for 15 min, *p*-nitrophenol amount released in the reaction was measured using Multiplate Reader. Orlistat was used with the same concentrations as a control. The results were expressed as percentage inhibition, which was calculated using the formula, **Inhibitory activity (%) = (1 − As/Ac) × 100,** where, **As** is the absorbance in the presence of test substance and **Ac** is the absorbance of control. The IC_{50} value was defined as the concentration of pancreatic lipase inhibitor to inhibit 50% of its activity under the assay conditions. Estimation of IC_{50} was done from dose response curve graphic plots for each conc. by using non-linear regression analysis of GraphPad Prism 5 software. Each experiment was performed in triplicates, and all values are represented as means ± standard deviation of triplicates.

3. Results and discussion

3.1. Structural identification of polyphenols and other constituents by UPLC-ESI-MS/MS

In this study, UPLC- ESI-MS/MS in both negative and positive ion modes was used to analyze TNC, TNE and TNB fractions of *T. nubica* for the first time. The identification of compounds based on their MS^2 data given by mass of the precursor ion and their fragments, together with neutral mass loss and known fragmentation patterns for the given classes of compounds as well as comparison with the available literature library search. The compounds were arranged according to retention time (R_t).

The distribution of the identified compounds in the three analyzed samples can be checked in Table 1 that lists the 107 compounds detected with UPLC-ESI-MS/MS in negative and positive modes. The table includes compounds' names, retention times' (R_t) of the assigned peaks, molecular ion value either $[M-H]^-$ or $[M + H]^+$ as well as MS^2 signals and used published references which helped to confirm the proposed identification of compounds in different tested fractions of *T. nubica*.

When using negative polarity in LC-MS analyses, the major signal found in the spectra was the pseudomolecular ion

Table 1 Metabolites identified in *T. nubica* aerial parts chloroform (TNC), ethyl acetate (TNE) and *n*-butanol (TNB) fractions using UPLC-ESI-MS/MS analysis in negative and positive ionization modes.

No.	Compound name	R_t (min)	$[M-H]^-$ (*m*/*z*)	$[M+H]^+$ (*m*/*z*)	MS^2 fragments (*m*/*z*)	TNC	TNE	TNB	Ref.
1	Oleuropein	0.82	539		377, 341, 307, 215, 179	+		+	(Zemmouri et al. 2014)
2	Tyrosol	0.82		121	103, 93, 77		+	+	(Lambert et al. 2015)
3	Succinic acid	1.12	117		117, 99, 73			+	(Jackson Seukep et al. 2020)
4	*p*-Hydroxybenzoic acid	1.78	137		93		+		(El-Sayed et al. 2017)
5	*p*-Hydroxy benzoic acid isomer	4.85		139	121, 111		+		(FooDB 2020)
6	Hydroxy methoxy benzoic acid hexoside (vanillic acid glucoside)	6.73	329		329, 167 $[M-H-162]^-$, 123			+	(Ancillotti et al. 2018)
7	Loliolide	7.04		197	179, 161, 135, 107	+	+	+	(Abu-Reidah et al. 2019)
8	Naringenin-7-*O*-glucoside	7.67	433		433, 271, 151, 119			+	(Jackson Seukep et al. 2020)
9	Succinic acid isomer	8.85	117		117, 99, 73	+			(Jackson Seukep et al. 2020)
10	Quercetin hexoside	8.95	463		301, 300			+	(Natić et al. 2015)
11	Succinic acid isomer	9.07	117		99, 73			+	(Jackson Seukep et al. 2020)
12	Hydroxy methoxy benzoic acid hexoside (vanillic acid glucoside) isomer	9.28	329		329, 167 $[M-H-162]^-$, 123			+	(Ancillotti et al. 2018)
13	Artonin G	9.34	503		475, 447			+	(Ye et al. 2019)
14	Syringaresinol *O*-D-glucopyranoside	9.51	579		417 $[M-H-162]^-$		+		(Ni et al. 2008)
15	Apigenin-*O*-glucoside	9.58	431		269 $[M-H-162]^-$, 225, 151			+	(Jackson Seukep et al. 2020)
16	*p*-Hydroxybenzoic acid isomer	9.76	137		93		+		(El-Sayed et al. 2017)
17	Peonidin-3-*O*-glucoside	10.01		463	301		+		(Lee et al. 2009)
18	Apigenin-*O*-hexoside	10.16		433	271, 153		+		(Abu-Reidah et al. 2019)
19	Kaempferl-3-*O*- rhamnoside (afzelin)	10.27		433	471*, 433, 287 $[M+H-146]^+$			+	(Jang et al. 2018)
20	kaempferol-3-*O*-galactoside (trifolin)	10.46		449	471**, 449, 287			+	(Jang et al. 2018)
21	Luteolin-7-*O*- glucoside	10.46	447		285, 257, 243		+	+	(Ziani et al. 2018)
22	kaempferol-3-*O*-galactoside (trifolin) isomer	10.62		449	471**, 449, 287		+	+	(Jang et al. 2018)
23	Luteolin-7-*O*- glucoside isomer	10.62	447		285, 257, 243		+	+	(Ziani et al. 2018)
24	Nonanedioic acid (Azelaic acid)	10.88	187		125, 97		+	+	(Jackson Seukep et al. 2020)
25	Kaempferol-3-*O*-	10.93	461		285		+		(Davis et al.

(*continued on next page*)

Table 1 (*continued*)

No.	Compound name	R_t (min)	$[M-H]^-$ (*m*/*z*)	$[M + H]^+$ (*m*/*z*)	MS^2 fragments (*m*/*z*)	TNC	TNE	TNB	Ref.
	glucuronide								2006)
26	6-Methyl brosimacutin D/ 6-Methyl brosimacutin E	10.93		355	337, 295, 283, 235, 217 (100%), 163		+		(Xu et al. 2012)
27	Dehydrocycloxanthohumol	11.21		353	233, 147	+			(Stevens et al. 1997)
28	5-Hydroxy-3,4′,7-trimethoxy-flavone	11.23	327		312, 297		+		(Simirgiotis et al. 2015)
29	Heterophyllin	11.85	503		285, 259, 243		+		(Ye et al. 2019)
30	Kaempferol-3-*O*-glucoside (astragalin)	12.46		449	471**, 287$[M + H-162]^+$		+	+	(Jang et al. 2018)
31	Kaempferol -*O*-dihexoside	12.47	609		285$[M-H-162–162]^-$			+	(Ziani et al. 2018)
32	Formononetin	12.61	267		252		+		(Clarke et al. 2008)
33	7,3′,4′-Trihydroxyflavone	12.68		271	243	+			(Aldini et al. 2011)
34	Heterophyllin isomer	13.37	503		285, 259, 243		+		(Ye et al. 2019)
35	Succinic acid isomer	13.49	117		99	+			(Jackson Seukep et al. 2020)
36	Genistein	13.58	269		133		+	+	(Singh et al. 2010)
37	Apigenin-*O*-hexoside isomer	13.60		433	271 $[M + H-162]^+$, 153		+	+	(Abu-Reidah et al. 2019)
38	Axillarin hexoside	13.76		509	449, 347, 303	+			(Bakr et al. 2016)
39	Hispidulin-7-*O*-hexoside	13.76	461		447, 299, 255	+			(Spínola et al. 2015)
40	Moracin F	13.90	285		285, 255, 213		+	+	(FooDB 2020)
41	Cirsimaritin (5,4′-dihydroxy-6,7-dimethoxyflavone)	14.10	313		298, 283		+		(Hossain et al. 2010)
42	Isorhamnetin	14.13		317	302, 168	+	+		(Abu-Reidah et al. 2019)
43	Scrophulein	14.51		315	300, 282, 254		+		(Abu-Reidah et al. 2019)
44	Daidzein	14.71		255	295 $[M + 2H + K]^+$, 278** 237, 199, 157, 137		+		(de Rijke 2005; Lee et al. 2005)
45	Chrysin hexoside	14.71	415		415, 253$[M-H-162]^-$, 209		+		(FooDB 2020) (Fabre et al. 2001)
46	Dehydrocycloxanthohumol isomer	15.09		353	233, 147	+			(Stevens et al. 1997)
47	Hydroxy methoxy benzoic acid hexoside (vanillic acid glucoside) isomer	15.20	329		329, 167 $[M-H-162]^-$, 123		+		(Ancillotti et al. 2018)
48	Glucaric acid derivative	15.45	425		327, 209	+			(Spínola et al. 2015)
49	Nonanedioic acid (Azelaic acid) isomer	15.50	187		187, 125, 97			+	(Jackson Seukep et al. 2020)
50	(-)-Pinellic acid	15.56	329		329, 311, 229, 211, 171, 139, 99		+		(Jackson Seukep et al. 2020)
51	Lactuside B	15.67		429	231, 185, 175, 157	+			(Abu-Reidah et al.

Table 1 (*continued*)

No.	Compound name	R_t (min)	$[M-H]^-$ (*m*/*z*)	$[M+H]^+$ (*m*/*z*)	MS^2 fragments (*m*/*z*)	TNC	TNE	TNB	Ref.
									2019)
52	Carnosol	15.91	329		285	+			(Hossain et al. 2010)
53	(+)- Catechin	15.92		291	273, 249, 165, 151, 139, 123, 119		+		(Aldini et al. 2011)
54	(-)-Pinellic acid isomer	16.01	329		329, 311, 229, 211, 171, 139, 99			+	(Jackson Seukep et al. 2020)
55	Cinnamic acid-*O*-xylosylhexoside	16.14	487		548 $[M-2H+Na+K]^-$, 509 $[M-2H+Na]^-$, 441, 293	+			(Spínola et al. 2015)
56	Corylidin	16.14		369	391**, 323, 309, 297, 295, 281, 269		+		(Xu et al. 2012)
57	Dehydrocycloxanthohumol isomer	16.17		353	233, 147	+			(Stevens et al. 1997)
58	(-)-Pinellic acid isomer	16.32	329		329, 311, 229, 211, 171, 139, 99		+	+	(Jackson Seukep et al. 2020)
59	Artonin G isomer	16.53	503		447			+	(Ye et al. 2019)
60	Corosolic acid	16.72	471		427		+		(Abu-Reidah et al. 2019)
61	Euchrenone a7 malonate	17.11		427	341$[M+H-86]^+$, 205, 163, 149, 145, 135, 121, 117, 93, 69, 65	+	+		(Xu et al. 2012)
62	Glucaric acid derivative	17.13	425		327, 209	+			(Spínola et al. 2015)
63	Cinnamic acid-*O*-xylosylhexoside isomer	17.35	487		548 $[M-2H+Na+K]^-$, 509 $[M-2H+Na]^+$, 441, 293	+			(Spínola et al. 2015)
64	Psorachalcone A	17.35		341	269, 221, 203, 175, 161, 149, 147, 121, 119, 93	+	+	+	(Xu et al. 2012)
65	Glucaric acid derivative	17.94	425		327, 209	+	+	+	(Spínola et al. 2015)
66	Bakuchiol	17.94		257	145, 133, 121, 107, 81, 69	+	+		(Xu et al. 2012)
67	Kaempferol hexoside glucuronide	18.36		625	449, 287	+	+		(Bakr et al. 2016)
68	(-)-Pinellic acid isomer	18.47	329		329, 311, 229, 211, 171, 139, 99		+	+	(Jackson Seukep et al. 2020)
69	Linoleic acid	18.50	279		261	+			(Della Corte et al. 2015)
70	(-)*cis*-Rotenolone	18.81		411	393, 381, 378, 367, 257, 207, 187, 143, 139, 109, 85, 81, 43	+	+		(FooDB 2020) (Caboni et al. 2008)
71	Oxooctadecadienoic acid	19.42	293		275, 235	+			(Abu-Reidah et al. 2019)
72	Moracin L	19.47	323		323, 255, 225	+			(FooDB 2020)
73	Naringenin-*O*-diglucoside	19.50	595		433[M-H-162]$^-$, 313, 271[M-H-162–162]$^-$, 177		+		(Jackson Seukep et al. 2020)
74	Quercetin	19.75	301		227, 151	+			(Hossain et al. 2010)
75	Dimethyl rosmarinic acid glucuronide	19.81	563		387, 359	+			(Achour et al. 2018)
76	Bakuchalcone/ bavachromanol	20.19		341	221, 203, 163, 161	+			(Xu et al. 2012)
77	13*S*-Hydroxyoctadecadienoic	20.25	295		295, 251	+			(Jackson Seukep et al.

(*continued on next page*)

Table 1 (*continued*)

No.	Compound name	R_t (min)	$[M-H]^-$ (*m*/*z*)	$[M + H]^+$ (*m*/*z*)	MS^2 fragments (*m*/*z*)	TNC	TNE	TNB	Ref.
	acid								2020)
78	Oxooxtadecadienoic acid isomer	20.52	293		275, 235		+		(Abu-Reidah et al. 2019)
79	13-Keto-9*Z*,11*E*-octadecadienoic acid	20.68	293		293, 265	+	+	+	(Jackson Seukep et al. 2020)
80	13*S*-Hydroxyoctadecadienoic acid isomer	21.15	295		295, 251	+	+	+	(Jackson Seukep et al. 2020)
81	Myricetin	21.19		319	277, 263, 245, 153		+	+	(de Rijke 2005)
82	(-)-Epicatechin	21.69		291	331 $[M + H_2O + Na]^+$, 291		+		(Jang et al. 2018)
83	7,3′,4′-Trihydroxyflavone isomer	21.80		271	243	+			(Aldini et al. 2011)
84	Moracin O	23.18	325		325, 293			+	(FooDB 2020)
85	Gancaonin A / Gancaonin M	23.31		353	391*, 375**, 297, 285, 269, 221, 69		+		(Xu et al. 2012)
86	6-Prenylnaringenin derivative	23.90	517		339, 219	+		+	(Clarke et al. 2008)
87	Artoindonesianin *I*	24.09	505		447, 285		+		(Ye et al. 2019)
88	Psoralenol	24.24		339	377*, 321, 279 , 267, 251, 239, 223, 137	+	+		(Xu et al. 2012)
89	Lanopalmitic acid	24.36	271		225	+	+	+	(Abu-Reidah et al. 2019)
90	3-(6-malonyl-glucopyranosyl)-rosmarinic acid	24.89		609	361	+			(Abu-Reidah et al. 2019)
91	Gancaonin A / Gancaonin M isomer	25.06		353	391*, 375**, 297, 285, 269, 221, 69	+	+	+	(Xu et al. 2012)
92	Cohumulone	25.24	347		278	+			(Quifer-Rada et al. 2015)
93	Quercetin isomer	25.37		303	179, 151	+			(Abu-Reidah et al. 2019)
94	Isoxanthohumol	25.82		355	299, 235, 179, 147		+		(Stevens et al. 1997)
95	Ethyl myristate	26.31	255		255	+	+	+	(Jackson Seukep et al. 2020)
96	7,3′,4′-Trihydroxyflavone isomer	26.31		271	243	+	+		(Aldini et al. 2011)
97	Oleic acid	26.74	281		281	+	+	+	(Jackson Seukep et al. 2020)
98	Icariside E7	27.09		595	351, 207	+	+		(Abu-Reidah et al. 2019)
99	Morachalcone A	27.47		341	382 $[M + H + H_2O + Na]^+$, 380*, 359 $[M + H + H_2O]^+$, 267 $[M + H\text{-}74]^+$, 149	+	+	+	(Seo et al. 2015)
100	Apigenin	28.25		271	271, 153		+		(Abu-Reidah et al. 2019)
101	Oleic acid isomer	28.43	281		281		+		(Jackson Seukep et al.

Table 1 (*continued*)

No.	Compound name	R_t (min)	$[M-H]^-$ (*m/z*)	$[M+H]^+$ (*m/z*)	MS^2 fragments (*m/z*)	TNC	TNE	TNB	Ref.
102	Naringenin	28.47	271		187, 151			+	2020) (Chen et al. 2015)
103	Conidendrin	29.17	355		340 $(M-H-CH_3)^-$, 337 $(M-H-H_2O)^-$, 322, 310 $(M-H-CH_2-O-CH_3)^-$, 295		+	+	(Sanz et al. 2012)
104	Ethyl myristate isomer	29.44	255		255			+	(Jackson Seukep et al. 2020)
105	Cistanoside F	30.48	487		487, 179, 161, 135	+			(Sanz et al. 2012)
106	Ethyl myristate isomer	31.11	255		255	+			(Jackson Seukep et al. 2020)
107	Dimethyl rosmarinic acid	31.23	387		359	+			(Achour et al. 2018)

*= Potassium adduct; **= Sodium adduct; R_t = Retention time; Ref. = Reference; TNC = Chloroform; TNE = Ethyl acetate; TNB = *n*-

$[M-H]^-$. On the contrary, in positive ion mode, in many cases $[M+H]^+$ was not the usual MS signal; water losses were very common ($[M+H\text{-}H_2O]^+$) and alkali adducts (mainly $[M+Na]^+$ and $[M+K]^+$) were also regularly existed.

3.1.1. Phenolic derivatives

Tyrosol (**2**) was characterized by two fragments *m/z* 93; corresponding to the phenol group and *m/z* 77; corresponding to the aromatic ring, respectively (Lambert et al. 2015). Tyrosol showed a protonated molecular ion at *m/z* 121 that not refer to the $[M+H]^+$ ion, but to the $[M-H_2O+H]^+$ according to Lambert et al. (2015)

Succinic acid (**3**) and its isomers (**9, 11 and 35**) (Jackson Seukep et al. 2020) and *p*-hydroxybenzoic acid (**4**) and its isomers (**5** and **16**) (El-Sayed et al. 2017; FooDB 2020) were recognized by comparing its MS^2 fragmentation pattern with the previously reported data.

The LC–ESI–MS/MS spectra of the molecular ion peak $[M-H]^-$ at *m/z* 329 gave the fragment ion at *m/z* 167 that indicate the neutral loss for one glucose moiety (162 Da) assigned a hydroxy methoxy benzoic acid hexoside that known as vanillic acid glucoside (**6**) and its isomers (**12, 47**) (Ancillotti et al. 2018).

Azelaic acid (nonanedioic acid) (**24**) and its isomer (**49**) which are dicarboxylic acids were identified (Jackson Seukep et al. 2020).

Compound **55** and its isomer (**63**) exhibited molecular ion at *m/z* 487 in MS spectrum. However, the product ion in MS/MS spectrum was at *m/z* 293 $[M+H\text{-}162\text{–}132]^+$ corresponding to cinnamic acid in structure and to the neutral loss of hexosyl (162 Da) and xylosyl (132 Da) moieties. Therefore, the compound was assigned to cinnamic acid-*O*-xylosylhexoside (Spínola et al. 2015).

Three rosmarinic acid derivatives were detected in the chloroform fraction of *T. nubica*. The precursor ion of compound **75** was detected at *m/z* 563 $[M-H]^-$ and its characteristic MS^2 fragment ions at *m/z* 387 $[M-H-176]^-$ suggesting the neutral loss of glucuronide moiety (176 Da) and at *m/z* 359 related to deprotonated rosmarinic acid and consequently it was tentatively identified as dimethyl rosmarinic acid glucuronide, while compound **107** produced a pseudomolecular ion at *m/z* 387 with main MS^2 fragment at *m/z* 359 and was tentatively identified as dimethyl rosmarinic acid (Achour et al. 2018). Compound **90** was identified as 3-(6-malonyl-glucopyranosyl)-rosmarinic acid (MS^1 at *m/z* 609 $[M+H]^+$, MS^2 at *m/z* 361 $[M+H\text{-}176\text{–}86]^+$ revealing the loss of glucuronide (176 Da) and malonyl (86 Da) moieties) (Abu-Reidah et al. 2019).

Cohumulone (**92**) (Quifer-Rada et al. 2015) and conidendrin (**103**) (Sanz et al. 2012) were annotated by matching with previous reports. Additionally, the peak eluting at R_t 30.48 min was tentatively assigned to a phenylethanoid derivative, which has been described as cistanoside F (**105**). Its fragmentation pattern was characterized by a major signal at *m/z* 179 $[M-H-\text{caffeoyl}-\text{rhamnosyl}]^-$, *m/z* 161 corresponding to further loss of water molecule and at *m/z* 135 $[\text{caffeic acid-}CO_2]^-$ (Sanz et al. 2012).

3.1.2. Lignans

Syringaresinol-*O*-*D*-glucopyranoside (**14**) (Ni et al. 2008) and icariside E7 (**98**) (Abu-Reidah et al. 2019) were identified by LC-MS as previously published.

3.1.3. Fatty acids

The compounds tentatively annotated as fatty acid derivatives, were showed only in negative mode. The fatty acids found were a (-)-pinellic (**50**), its isomers (**54**, **58** and **68**), 13S-hydroxyoctadecadienoic (**77**), its isomer (**80**), 13-keto-9Z,11E-octadecadienoic (**79**), ethyl myristate (**95**), its isomers (**104**, **106**), oleic (**97**), its isomer (**101**) (Jackson Seukep et al. 2020), linoleic (**69**) (Della Corte et al. 2015) oxooctadecadienoic (**71**), its positional isomer (**78**) and lanopalmitic acid (**89**) (Abu-Reidah et al. 2019).

3.1.4. Flavonoids

3.1.4.1. Flavanones. Six flavanones (**8, 26, 61, 73, 86, 102**) were identified in the evaluated samples (four of them were in negative ionization mode and the other two were in positive mode).

Compound **26** with $[M + H]^+$ at *m/z* 355 was tentatively assigned as 6-methylbrosimcutin D/ 6-methylbrosimcutin E showing daughter ions at *m/z* 337, 295, 283, by successive diagnostic losses of H_2O (18 Da), C_3H_8O (60 Da) and C_4H_8O (72 Da), respectively that yielded from a 2,2-dimethyl-3-hydro xydihydropyran ring suggesting that there was a mono-hydroxy-prenyl group in its structure **(**Xu et al. 2012**)**. Compound **61** with a protonated ion at *m/z* 427 was tentatively assigned as euchrenone a7 malonate (7,2′,4′-trihydroxy-8-iso prenylflavanone malonate) with main MS^2 fragment ion at *m/z* 341 $[M + H\text{-}86]^+$ corresponding to loss of a malonic acid moiety (86 Da) and producing identical product ions as euchrenone a7 **(**Xu et al. 2012**)**.

Two naringenin glycosides, naringenin-7-*O*-glucoside (**8**) and naringenin-*O*-diglucoside (**73**), were detected at R_t 7.67 and 19.50 min **(**Jackson Seukep et al. 2020**)**. Compound **86** with $[M-H]^-$ at *m/z* 517 was characterized as a 6-prenylnaringenin derivative showing typical aglycone at *m/z* 339 **(**Clarke et al. 2008**)**. Naringenin (**102**) was recognized by comparing its MS^2 fragmentation pattern with the previously reported data **(**Chen et al. 2015**)**.

3.1.4.2. Flavonols. Five flavonols were detected in examined fractions. Quercetin hexoside was proposed for compound **10** at R_t 8.95 min (*m/z* 463, $[M-H]^-$). In the MS^2 spectrum, a fragment ion at *m/z* 301, which corresponds to quercetin in structure after hexose unit loss **(**Natić et al. 2015**)**. Quercetin (**74**) and its isomer (**93**) were recognized by comparing its MS/MS fragmentation pattern with the previously reported data either in negative ionization mode **(**Hossain et al. 2010**)** or positive mode **(**Abu-Reidah et al. 2019**)**, respectively.

Compound **38** showed mass spectrum with a precursor ion at *m/z* 509 $[M + H]^+$. This precursor ion showed MS/MS spectrum with a product ion at *m/z* 449 $[M-H-60]^-$ after the neutral loss of two methoxy moieties (60 Da) and MS^2 fragment at *m/z* 347 $[M + H\text{-}162]^+$ suggesting the neutral loss of hexose moiety and was tentatively identified as axillarin hexoside (axillaroside) **(**Bakr et al. 2016**)**. Compound related to peak **42** was identified as isorhamnetin. It exhibited a protonated molecular ion at *m/z* 317 **(**Abu-Reidah et al. 2019**)**

3.1.4.3. Flavones. For compounds **13** and **59,** the neutral loss of 56 Da (C_4H_8 unit) from $[M\text{-}H]^-$ ion at *m/z* 503 to produce ion peak at *m/z* 447 and loss of 28 Da (CO unit) from deprotonated molecular ion to produce ion peak at *m/z*475, suggested that these compounds identified as prenylated flavonoid known as artonin G **(**Ye et al. 2019**)**.

Four apigenine derivatives were detected. Compound **15** with $[M-H]^-$ at *m/z* 431 was characterized as apigenin-*O*-glucoside showing typical aglycone at *m/z* 269 after loss of 162 mass units (glucosyl moiety) **(**Jackson Seukep et al. 2020**)**. Additionally compound **18** and its isomer (**37**) showed a protonated pseudomolecular ion at *m/z* 433 (MS^2 at *m/z* 271 $[M + H-glc.]^+$ which have been described as apigenin-*O*-hexoside, while apigenin aglycone (**100**) was identified as previously published **(**Abu-Reidah et al. 2019**)** and it was considered as a major compound in $TNE^{(+)}$ fraction. Luteolin-7-*O*-glucoside was proposed for compounds **21** and **23** as previously reported **(**Ziani et al. 2018**)** and it was represented as the major compound in *n*-butanol spectrum (in negative mode)**.**

Seven kaempferol derivatives were detected. Kaempferol-3-*O*-glucuronide (**25**) **(**Davis et al. 2006**)**, and kaempferol-*O*-dihexoside (**31**) **(**Ziani et al. 2018**)**, kaempferol-3-*O*-rhamnoside (afzelin) (**19**) were tentatively identified by neutral loss of 176 Da (glucuronide moiety), 324 Da (two hexosyl moiety), 146 Da (rhamnosyl moiety), respectively. While kaempferol-3-*O*-galactoside (trifolin) (**20**), its isomer (**22**), and kaempferol-3-*O*-glucoside (astragalin) (**30**) **(**Jang et al. 2018**)** were identified by neutral loss of 162 Da (galactose or glucose moieties). Kaempferol hexoside glucuronide (**67**) was identified by loss of 176 Da (glucuronyl moiety) and additional loss of 162 Da (hexosyl moiety) **(**Bakr et al. 2016**)**.

Compound **28**, showed a deprotonated molecular ion at *m/z* 327 producing daughter fragment ions at *m/z* 312 $[M-H-CH_3]^-$ and *m/z* 297 $[M-H-2CH_3]^-$, was identified as 5-hydroxy-3,4′,7-trimethoxy flavone **(**Simirgiotis et al. 2015**)**. 5,4′-dihydroxy-6,7-dimethoxyflavone that is known as cirsimaritin (**41**) **(**Hossain et al. 2010**)** was identified as previously published in negative ionization mode while scrophulein (**43**), which is known as cirsimaritin, was detected in positive ionization mode **(**Abu-Reidah et al. 2019**)**.

Heterophyllin (**29**)**,** its positional isomer **(34)** and artoindonesianin *I* **(87)** were identified in the ethyl acetate fraction by the comparison of their MS spectrum in full scan mode and MS/MS spectrum with the published data **(**Ye et al. 2019**)**. Chrysin hexoside (**45**) **(**Fabre et al. 2001**)** and hispidulin-7-*O*-hexoside (**39**) **(**Spínola et al. 2015**)** were tentatively identified as previously published. Three isomers (**33, 83** and **96**) with a molecular ion at *m/z* 271 in ESI^+ mode were tentatively identified as 7,3′,4′-trihydroxyflavone **(**Aldini et al. 2011**)**. Myricetin (3,5,7,3′,4′,5′-hexahydroxyflavone) was proposed for the compound **81 (**de Rijke 2005**)**.

3.1.4.4. Isoflavones. Six isoflavones such as formononetin (**32**), genistein (**36**), daidzein (**44**), gancaonin A/gancaonin M (**85, 91**) and psoralenol (**88**) were identified. The major compound in ethyl acetate spectrum was formononetin (**32**) (7-hydroxy-4′-methoxy isoflavone) that showed a $[M-H]^-$ at *m/z* 267 producing a daughter fragment ion at *m/z* 252 $[M-H-CH_3]^-$ **(**Clarke et al. 2008**)**. Genistein (**36**) (5,7,4′-trihydroxy isoflavone) **(**Singh et al. 2010**)** and daidzein (**44**) **(**Lee et al. 2005; de Rijke 2005**)** were identified as previously published.

Compounds **85**, **88** and **91** were identified as prenylated isoflavonoids. Gancaonin A / gancaonin M (**85**) and its isomer (**91**) have one prenyl chain in its structure which was evidenced by a characteristic fragment ion at *m/z* 69 of the isoprene (C_5H_9) moeity in addition to presence of daughter ion at *m/z* 297 $[M + H\text{-}56]^+$ due to the neutral loss of C_4H_8 (56 Da) moiety **(**Xu et al. 2012; Seo et al. 2015**)**. Gancaonin A / gancaonin M was the major compound in $TNC^{(+)}$ and $TNE^{(+)}$ spectra.

Psoralenol (**88**) showed MS^1 at *m/z* 339 $[M + H]^+$, MS^2 at *m/z* 267 $[M + H\text{-}72]^+$, 279 $[M + H\text{-}60]^+$ and 321 $[M + H\text{-}18]^+$ revealing the loss of C_4H_8O (72 Da), C_3H_8O (60 Da) and H_2O (18 Da) moieties that indicated that this compound contains 2,2-dimethyl-3-hydroxydihydropyran ring. In addition to MS^2 peak at *m/z* 137 that suggest the presence of mono-hydroxy-prenyl group in ring A **(**Xu et al. 2012**)**.

3.1.4.5. Flavanols. Flavanols as (+)- catechin (**53**) **(**Aldini et al. 2011**)** and (-)- epicatechin (**82**) **(**Jang et al. 2018**)** with $[M + H]^+$ at *m/z* 291 for both of them were identified in positive ionization mode in tested ethyl acetate fraction as previously published.

3.1.5. Chalcones

Seven chalcones were described in different fractions of *T. nubica* in LC-ESI-MS-MS positive mode. Dehydrocycloxanthohumol (**27**), its isomers (**46** and **57**), isoxanthohumol (**94**) (Stevens et al. 1997), bakuchalcone/ bavachromanol (**76**), psorachalcone A (**64**) (Xu et al. 2012) and morachalcone A (**99**) (Seo et al. 2015) were confirmed by comparing their MS/MS spectra with those of reported data. Morachalcone A (**99**) was the major compound in *n*-butanol fraction.

3.1.6. Terpenoid derivatives

Carnosol proposed for compound **52** (m/z 329, $[M-H]^-$) (Hossain et al. 2010), while corosolic acid is proposed for compound **60** (m/z 471, $[M-H]^-$) (Abu-Reidah et al. 2019) and bakuchiol (**66**) (Xu et al. 2012) as monoterpene phenol were identified as previously reported. Bakuchiol was the major compound in chloroform fraction.

3.1.7. Anthocyanins

Compound **17** was tentatively identified as peonidin-3-*O*-glucoside as it exhibited $[M + H]^+$ ion at m/z 463 and MS^2 base peak ion at m/z 301 $[M + H\text{-}162]^+$ after the neutral loss of glucosyl moiety (162 Da) (Lee et al. 2009).

3.1.8. Benzofurane compounds

In negative mode analysis, three benzofurane derivatives were identified, moracin F (**40**), moracin L (**72**) and moracin O (**84**) with $[M-H]^-$ at m/z 285, 323 and 325, respectively (FooDB 2020) while in positive ionization mode only loliolide (**7**) as benzofurane derivative with $[M + H]^+$ at m/z 197 was detected (Abu-Reidah et al. 2019).

3.1.9. Miscellaneous compounds

Oleuropein (**1**) showed a deprotonated pseudomolecular ion at m/z 539 (MS^2 at m/z 377 $[M-H-glc.]^-$ and 307 $[M-H-glc.\text{-}C_4H_6O]^-$) (Zemmouri et al. 2014). Oleuropein was previously reported to be identified in Tephrosia (Nigam and Arnold 2018). Glucaric acid derivatives (**48, 62, 65**) with $[M + H]^+$ at m/z 425 were identified in negative ionization mode as major compound in tested chloroform fraction (Spínola et al. 2015).

In positive mode analysis, one sesquiterpene lactone known as lactuside B (**51**) with $[M + H]^+$ at m/z 429 (Abu-Reidah et al. 2019), one rotenoid known as (-)*cis*-rotenolone (**70**) with $[M + H]^+$ at m/z 411 (Caboni et al. 2008; FooDB 2020) were detected. As well as, one coumarin compound, corylidin (**56**), with $[M + H]^+$ at m/z 369 and MS^2 fragments at m/z 309 $[M + H\text{-}60]^+$ corresponding to loss of $C_2H_4O_2$ and at m/z 297 $[M + H\text{-}72]^+$ corresponding to loss of C_4H_8O (Xu et al. 2012) was detected.

3.2. The antioxidant activity

Antioxidants are able to decrease, delay or maybe inhibit the oxidative damage through scavenging of free radicals. These reactive oxygen species play a vital role within the pathogenesis of various diseases like cancer, hypertension, diabetes, atherosclerosis, and inflammatory disease (Sharma et al. 2018; Vladimir-Knežević et al. 2011). Polyphenols especially flavonoids are one of the most important natural antioxidants which are widely distributed in various plant families including Fabaceae. This family includes many species which are valuable sources of natural antioxidants (Hanganu et al. 2010).

Plants fortified with antioxidants, such as isoflavonoid, can also be regarded as an alternative method for handling and treating chronic diseases linked to oxidative stress (de Mendonça et al. 2020).

It was reported that flavonoids are strong free radical scavengers as they are able to donate hydrogen from their phenolic groups (Hanna 2011; Tripoli et al. 2007). The flavonoids antioxidant activity is related to the presence of catechol structure (3′, 4′ hydroxyl groups) in the B ring which enhances lipid peroxidation inhibition. Additionally, the presence of 2, 3-double bond in conjugation with the carbonyl group and the hydroxyl groups in C3 and C5 increase the antioxidant activity of flavonoids (Heim et al. 2002; Tripoli et al. 2007). On the other hand, the absence of the hydroxyl group attached to C3 in flavonones decreases the antioxidant activity (Hanna 2011; Tripoli et al. 2007). (**See** Fig. 1)

In the present research, series of concentrations ranged from 5 to 320 μg/mL in methanol were used. The DPPH scavenging percentage of TNC, TNE and TNB as well as ascorbic acid as standard and SC_{50} values (the concentration required to scavenge DPPH by 50%) are presented in Fig. 2 A and B, respectively. All of them showed a concentration-dependent antioxidant activity as demonstrated by increase in their DPPH radical scavenging activity. The smaller the SC_{50} the higher the scavenging activity is. The tested fraction or compound is considered as a very strong antioxidant when SC_{50} values < 50, strong (50–100), moderate (100–150), and weak (151–200) µg/mL (Winarsi and Yuniaty 2019) Therefore, according to the SC_{50} values, all the tested fractions of *T. nubica* (TNE, TNC, and TNB) showed a moderate antioxidant activity with SC_{50} 139.9 ± 0.8, 144.9 ± 1.5 and 148.9 ± 1.3 µg/mL respectively compared to ascorbic acid 14.2 ± 0.5 µg/mL.

TNE exhibited the highest antioxidant activity compared to the other two tested fractions as indicated by its high DPPH scavenging percentage (68%) at 320 µg/mL and low SC_{50} values (139.9 ± 0.8 µg/mL). Its activity can be attributed to the presence of monoterpene phenol (bakuchiol) (Ma et al. 2020) and polyphenolic compounds such as phenolic acids and flavonoids (i.e., *p*-hydroxybenzoic acid, vanillic acid glucoside, formononetin, apigenin, kaempferol-3-*O*-glucuronide, genistein and artoindonesianin *I*).

During this study, bakuchiol and many major flavonoids were detected in LC-MS analysis of TNE (formononetin, apigenin, kaempferol-3-*O*-glucuronide, genistein and artoindonesianin *I*). Correlation between radical scavenging ability, SC_{50} values, and the identified phenolic acids and flavonoids in LC-MS analysis is considerable as extracts with higher flavonoids and/or phenolics contents showed higher antioxidant activity and lower SC_{50} value. These results are in accordance with the previous reports about the antioxidant properties of many *Tephrosia* species (Egharevba et al. 2019; Sindhu et al. 2017; Martinez et al. 2012; Hanganu et al. 2010).

3.3. The cytotoxic activity

The risk of neoplasia is increasing worldwide with higher mortality rates every year. Breast cancer is the main cause of cancer death among females that is responsible for 15–25% of all cancer cases and deaths. Liver cancer is much more common in

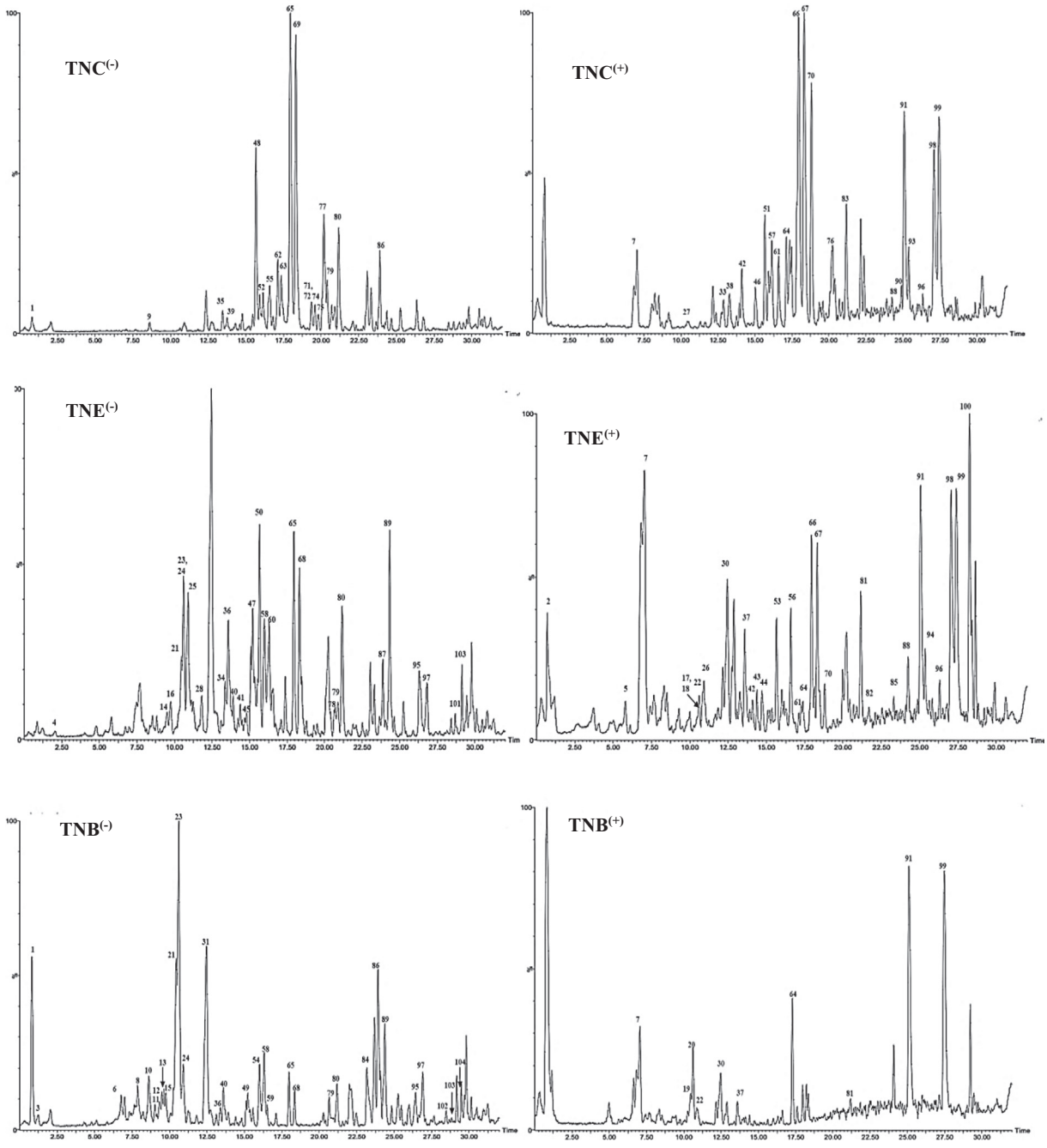

Fig. 1 UPLS-ESI-MS chromatograms of *T. nubica* aerial parts chloroform (TNC), ethyl acetate (TNE) and *n*-butanol (TNB) fractions in negative (−) and positive (+) ionization modes.

males. Furthermore, it is the second major cause of cancer death in men all over the world especially in underdeveloped countries (Torre et al. 2015). Recently, natural products and plant-derived compounds have attracted the attention of many researchers as a promising cancer therapy (Al-Abbasi et al. 2016; Solowey et al. 2014; Wannes et al. 2017).

The *in-vitro* cytotoxic activity *T. nubica* (TNC, TNE, and TNB) fractions against HepG-2 (hepatocellular carcinoma) and MCF-7 (breast carcinoma) using MTT assay and cisplatin as a positive standard was also studied. The rule used to evaluate the activity of *T. nubica* fractions depends on the IC_{50} values as reported by (Srisawat et al. 2013)). The tested fraction is considered as highly active when IC_{50} = 20 μg/mL, moderately active, IC_{50} = 21–200 μg/mL, weakly active IC_{50} = 20 1–500 μg/mL and inactive IC_{50} > 501 μg/mL.

According to the IC_{50} values, all the tested fractions of *T. nubica* (TNC, TNE, and TNB) as shown in (Fig. 2 **C & D and** Table 2), showed a decline in the cell viability in a dose-dependent manner against HepG-2 and MCF-7 cells. The ethyl acetate and chloroform fractions showed more significant cyto-

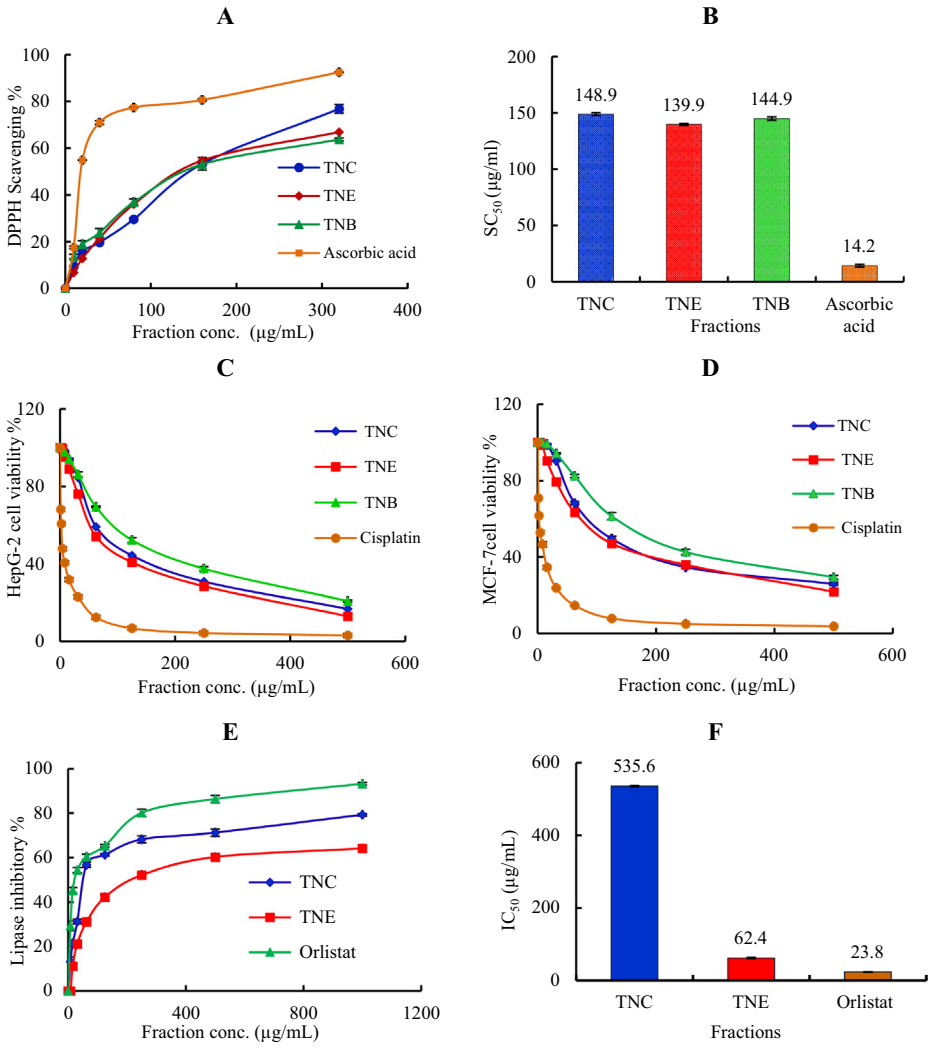

Fig. 2 **(A):** 2,2-diphyenyl-picrylhydrazyl (DPPH) radical scavenging activity of different concentrations (5–320 µg/mL) of *T. nubica* fractions. Data are presented as averages ± standard deviations from three experiments. **(B):** SC_{50} of antioxidant activity of *T. nubica* fractions and ascorbic acid. **(C):** Cytotoxic activity of *T. nubica* fractions against HepG-2 cell line at different concentrations **(D):** Cytotoxic activity of *T. nubica* fractions against MCF-7 cell line at different concentrations. **(E):** In vitro lipase inhibitory activity of *T. nubica* fractions compared to orlistat standard. **(F):** IC_{50} of anti-obesity activity of *T. nubica* fractions and orlistat. **TNC** (chloroform fraction), **TNE (**ethyl acetate fraction) and **TNB** (*n*-butanol fraction).

toxic activity against HepG-2 with IC_{50} 82.1 ± 3.1, 101 ± 2.8 µg/mL and MCF-7 with IC_{50} 114 ± 3.2, 124 ± 3. 9 µg/mL respectively. While *n*-butanol fraction showed moderate cytotoxicity against HepG-2 with IC_{50} 145 ± 7.9 µg/mL and a weak cytotoxic effect against MCF-7 with IC_{50} 201 ± 5.8 µg/mL compared to the other fractions (Table 2).

Table 2 Half maximum inhibitory concentration (IC_{50}) of (TNC, TNE, TNB) chloroform, ethyl acetate, and *n*-butanol fractions of *T. nubica* in cell viability of HepG-2 and MCF-7 cells after the treatment for 48 h, as measured by MTT assay. The data are presented as µg/mL.

Cell line	Tested fractions			
	IC_{50} (µg/mL)			
	TNC	TNE	TNB	Cisplatin
HepG-2 (Hepatocellular carcinoma)	101 ± 2.8	82.1 ± 3.1	145 ± 7.9	3.67 ± 3.8
MCF-7 (Breast carcinoma)	124 ± 3.9	114 ± 3.2	201 ± 5.8	5.71 ± 1.3

These are the mean of three determinations.

In case of HepG-2 cell line, the cytotoxicity of the applied fractions was arranged as follows: TNE > TNC > TNB. Unfortunately, TNB exhibited the weakest cytotoxic activity against HepG-2 cell line with IC_{50} of 145 ± 7.9 μg/mL when compared to cisplatin, 3.67 ± 3.8 μg/mL. The higher activity of TNE (IC_{50} = 82.1 ± 3.1 μg/mL) as a strong cytotoxic may be attributed to the presence of major compounds such as formononetin (de Mendonça et al. 2020).

Also, as indicated by IC_{50} values, the cytotoxicity of tested fractions against MCF-7 cell line is arranged as follow: TNE > TNC > TNB. A close cytotoxic effect was shown by TNE and TNC (IC_{50} 114 ± 3.2 and 124 ± 3.9 μg/mL, respectively).The cytotoxic activity of TNE may be attributed to formononetin as it was reported as a cytotoxic agent in a previous study (de Mendonça et al. 2020), and this cytotoxic activity may be enhanced by the presence of bakuchiol according to (Zhang et al. 2016)

This is the first report about the cytotoxic activity of *T. nubica* and these results are in agreement with the previous literatures about different *Tephrosia* species antitumor activities. The ethyl acetate fraction of *T. purpurea* showed hepatoprotective activity against CCl_4 induced hepatotoxicity in rats at doses of 50 mg/kg (Shah et al. 2011). Additionally, flavonoids isolated from the stems of *T. toxicaria* ethyl acetate fraction have cancer chemopreventive activity (Jang et al. 2003). Moreover, *T. calophylla*, *T. candida* and *T. tinctoria* have been studied using different cell lines (Ganapaty et al. 2009a; Ganapaty et al. 2009b; Parmar et al. 1988; Roy et al. 1986). In a different study the root extract of *T. calophylla* inhibited growth and induced apoptosis in the human breast carcinoma (Adinarayana et al. 2009). Investigation of the chloroform fraction of *T. nubica* in a previous study revealed the presence of prenylated flavones in addition to flavones and isoflavones. However, kaempferol 3,7 dirhamnoside, quercetin 3-galactoside 7-rhamnoside, and quercetin 3, 7 dirhamnoside, rotenone and deguelin were isolated from *T. nubica* methanolic extract (Sharaby and Ammar 1997).

The significant cytotoxic activity of the ethyl acetate and chloroform fractions of *T. nubica* in the current study may be attributed to the presence of bakuchiol and high flavonoidal content especially isoflavones.

3.4. The anti-obesity activity

Obesity is a serious worldwide health problem afflicting both developed and undeveloped countries and affecting all ages of populations. It is considered as a risk factor related to the development of different metabolic disorders such as hypertension, cardiovascular disease, type 2 diabetes, atherosclerosis and dyslipidemia (Zielinska-Blizniewska et al. 2019; Roh and Jung 2012). Currently, natural products and plant-derived compounds have attracted the attention for the obesity management by developing safe and efficient anti-obesity drugs (Nderitu et al. 2017).

Up to date nothing was reported about the anti-obesity activity of *T. nubica* growing in Saudi Arabia. In the present study screening of *T. nubica* ethyl acetate, chloroform and *n*-butanol fractions by pancreatic lipase inhibitory assay was carried out and shown in Fig. 2 **(E & F)**.

The results showed that TNE exhibited remarkable inhibitory activity than the TNC with IC_{50} 62.4 ± 1.5, 535.6 ± 2.1 μg/mL respectively. The IC_{50} value of ethyl acetate fraction (62.4 ± 1.5) is comparable with that of orlistat (23.8 ± 0.7). It was reported that organic acids (such as *p*-hydroxybenzoic acid) (Huang et al. 2015) and polyphenolic compounds (such as apigenin, formononetin, kaempferol-3-*O*-glucuronide, genistein and artoindonesianin *I*) (Yajima et al. 2005; Lei et al. 2007) in the plants are responsible for the anti-obesity activity. These compounds were detected as major compounds in TNE and absent in TNB chromatograms that may explaine why TNB fraction showed no anti-obesity activity.

Recently, the management of obesity by using natural compounds is not fully investigated and might be a significant substituent for producing harmless and efficient anti-obesity drugs (Nderitu et al. 2017). To the best of our knowledge, nothing was reported on the anti-obesity activity of *T. nubica*, so future studies are planned to isolate and purify the active compounds of *T. nubica* active fractions for further *in vivo* evaluation.

4. Conclusion

The current study represents the first research reporting the phytochemical constituents and pharmacological properties of *T. nubica*. Based on the results it could be concluded that the ethyl acetate fraction of *T. nubica* showed significant antioxidant, cytotoxic and anti-obesity activities compared to the other tested fractions. Finally, it might be an important natural alternative therapy especially for obesity treatment that makes it the good candidate for further anti-obesity drug development. Isolation of the major bioactive compounds from the most active fractions and investigation of their biological activities are planned in the further studies.

Declaration of Competing Interest

The authors declare that there are no conflicts of interest.

Acknowledgments

The authors thank Prof. Dr. Mohamed Yousef, Pharmacognosy Department, College of Pharmacy, King Saud University (KSU) for the plant identification.

Funding/support

This research did not receive any specific grant from funding agencies in the public, commercial, or not-for-profit sectors.

Authors' contributions

All authors made considerable contributions to the manuscript. HA, SA, WH, and ME designed the study. WH, HA, SA and ME performed the experiments. SA,WH and ME interpreted the results. ME, SA, HA, and WH wrote the manuscript. All authors revised the manuscript and confirmed it for publication.

References

Abu-Reidah, I.M., Arráez-Román, D., Al-Nuri, M., et al, 2019. Untargeted metabolite profiling and phytochemical analysis of *Micromeria fruticosa* L. (Lamiaceae) leaves. Food Chem. 279, 128–143.

Achour, M., Saguem, S., Sarriá, B., et al, 2018. Bioavailability and metabolism of rosemary infusion polyphenols using Caco-2 and HepG2 cell model systems. J. Sci. Food Agric. 98 (10), 3741–3751.

Adinarayana, K., Jayaveera, K., Madhu Katyayani, B., et al, 2009. Growth inhibition and induction of apoptosis in estrogen receptor positive and negative human breast carcinoma cells by *Tephrosia calophylla* roots. Pharm. Chem. J. 3, 35–41.

Al-Abbasi, F., Alghamdi, E., Baghdadi, M., et al, 2016. Gingerol synergizes the cytotoxic effects of doxorubicin against liver cancer cells and protects from its vascular toxicity. Molecules 21 (7), 886.

Al-Ghamdi, F., 2013. Morphological Diversity of Some Tephrosia Species (Fabaceae) in Saudi Arabia. Am. J. Plant Sciences 4 (3), 543–548.

Al Khateeb, W., Kanaan, R., El-Elimat, T., et al, 2017. In vitro propagation, genetic stability, and secondary metabolite analysis of wild lavender (*Lavandula coronopifolia* Poir.). Hortic. Environ. Biotechnol. 58 (4), 393–405.

Aldini, G., Regazzoni, L., Pedretti, A., et al, 2011. An integrated high resolution mass spectrometric and informatics approach for the rapid identification of phenolics in plant extract. J. Chromatogr. A 1218 (20), 2856–2864.

Ancillotti, C., Ulaszewska, M., Mattivi, F., et al, 2018. Untargeted metabolomics analytical strategy based on liquid chromatography/electrospray ionization linear ion trap quadrupole/orbitrap mass spectrometry for discovering new polyphenol metabolites in human biofluids after acute ingestion of *Vaccinium myrtillus* berry supplement. J. Am. Soc. Mass Spectrom. 30 (3), 381–402.

Bakr, R.O., Abd, S., Halim Mohamed, E., et al, 2016. Phenolic profile of *Centaurea aegyptiaca* l. Growing in egypt and its cytotoxic and antiviral activities. Afr. J. Tradit. Complement. Altern. Med. 6, 135–143.

Caboni, P., Sarais, G., Vargiu, S., et al, 2008. LC–MS–MS determination of rotenone, deguelin, and rotenolone in human serum. Chromatographia 68 (9–10), 739–745.

Chen, Y., Yan, T., Gao, C., et al, 2014. Natural products from the genus Tephrosia. Molecules 19 (2), 1432–1458.

Chen, Y., Yu, H., Wu, H., et al, 2015. Characterization and quantification by LC-MS/MS of the chemical components of the heating products of the flavonoids extract in Pollen typhae for transformation rule exploration. Molecules 20 (10), 18352–18366.

Clarke, D.B., Bailey, V., Lloyd, A., 2008. Determination of phytoestrogens in dietary supplements by LC-MS/MS. Food Addit. Contam. 25 (5), 534–547.

Davis, B.D., Needs, P.W., Kroon, P.A., et al, 2006. Identification of isomeric flavonoid glucuronides in urine and plasma by metal complexation and LC-ESI-MS/MS. J. Mass Spectrom. 41 (7), 911–920.

de Mendonça, M.A., Ribeiro, A.R., Lima, A.K.d. et al., 2020. Red propolis and its dyslipidemic regulator formononetin: evaluation of antioxidant activity and gastroprotective effects in rat model of gastric ulcer. Nutrients 12 (10):2951.

de Rijke, E., 2005. Trace-level determination of flavonoids and their conjugates: Application to plants of the Leguminosae family.

Della Corte, A., Chitarrini, G., Di Gangi, I.M., et al, 2015. A rapid LC–MS/MS method for quantitative profiling of fatty acids, sterols, glycerolipids, glycerophospholipids and sphingolipids in grapes. Talanta 140, 52–61.

Egharevba, G.O., Dosumu, O.O., Oguntoye, S.O., et al, 2019. Antidiabetic, antioxidant and antimicrobial activities of extracts of *Tephrosia bracteolata* leaves. Heliyon 5, (8) e02275.

El-Sayed, M.A., Al-Gendy, A.A., Hamdan, D.I., et al, 2017. Phytoconstituents, LC-ESI-MS Profile, antioxidant and antimicrobial Activities of *Citrus x limon* L. Burm. f. cultivar Variegated pink lemon. J. Pharmaceutical Sci. Res. 9 (4), 375.

Fabre, N., Rustan, I., de Hoffmann, E., et al, 2001. Determination of flavone, flavonol, and flavanone aglycones by negative ion liquid chromatography electrospray ion trap mass spectrometry. J. Am. Soc. Mass Spectrom. 12 (6), 707–715.

FooDB, 2020. The Metabolomics Innovation Centre https://foodb.ca/.

Ganapaty, S., Srilakshmi, G., Thomas, P.S., et al, 2009a. Cytotoxicity and antiprotozoal activity of flavonoids from three Tephrosia species. J. Natural Remedies 9 (2), 202–208.

Ganapaty, S., Srilakshmi, G.V.K., Pannakal, S.T., et al, 2009b. Cytotoxic benzil and coumestan derivatives from *Tephrosia calophylla*. Phytochemistry 70 (1), 95–99.

Gomha, S.M., Salah, T.A., Abdelhamid, A.O., 2015. Synthesis, characterization, and pharmacological evaluation of some novel thiadiazoles and thiazoles incorporating pyrazole moiety as anticancer agents. Monatsh. Chem. 146 (1), 149–158.

Gülçin, I., Küfrevioğlu, Ö.İ., Oktay, M., et al, 2004. Antioxidant, antimicrobial, antiulcer and analgesic activities of nettle (Urtica dioica L.). J. Ethnopharmacol. 90 (2–3), 205–215.

Hanganu, D., Vlase, L., OLAH, N., 2010. Phytochemical analysis of isoflavons from some Fabaceae species extracts. Notulae Botanicae Horti Agrobotanici Cluj-Napoca 38 (1):57-60.

Hanna, E.S.R., 2011. Isolation and structure elucidation of two diastereoisomeric prenylated flavonoids from *Tephrosia apollinea* root and their Chemotaxonomic Significance. The University of Khartoum, Khartoum, Sudan, Master Master.

Hassan, W.H., Abdelaziz, Sahar, Yousef, Al, Hanan, M., 2019. Chemical composition and biological activities of the aqueous fraction of *Parkinsonea aculeata* L. Growing in Saudi Arabia. Arabian J. Chem. 12 (3), 377–387.

Heim, K.E., Tagliaferro, A.R., Bobilya, D.J., 2002. Flavonoid antioxidants: chemistry, metabolism and structure-activity relationships. J. Nutritional Biochemistry 13 (10), 572–584.

Hossain, M.B., Rai, D.K., Brunton, N.P., et al, 2010. Characterization of phenolic composition in Lamiaceae spices by LC-ESI-MS/MS. J. Agric. Food. Chem. 58 (19), 10576–10581.

Huang, T.-W., Chang, C.-L., Kao, E.-S., et al, 2015. Effect of *Hibiscus sabdariffa* extract on high fat diet–induced obesity and liver damage in hamsters. Food & nutrition research 59 (1), 29018.

Jackson Seukep, A., Zhang, Y.-L., Xu, Y.-B., et al, 2020. *In vitro* antibacterial and antiproliferative potential of *Echinops lanceolatus* Mattf. (Asteraceae) and identification of potential bioactive Compounds. Pharmaceuticals (Basel) 13 (4), 59.

Jang, D.S., Park, E.J., Kang, Y.-H., et al, 2003. Potential cancer chemopreventive flavonoids from the stems of *Tephrosia toxicaria*. J. Nat. Prod. 66 (9), 1166–1170.

Jang, G.H., Kim, H.W., Lee, M.K., et al, 2018. Characterization and quantification of flavonoid glycosides in the Prunus genus by UPLC-DAD-QTOF/MS. Saudi J. Biological Sci. 25 (8), 1622–1631.

Kim, Y.S., Lee, Y.M., Kim, H., et al, 2010. Anti-obesity effect of *Morus bombycis* root extract: anti-lipase activity and lipolytic effect. J. Ethnopharmacol. 130 (3), 621–624.

Lambert, M., Meudec, E., Verbaere, A., et al, 2015. A high-throughput UHPLC-QqQ-MS method for polyphenol profiling in rosé wines. Molecules 20 (5), 7890–7914.

Lee, J.H., Kang, N.S., Shin, S.-O. et al., 2009. Characterisation of anthocyanins in the black soybean (Glycine max L.) by HPLC-DAD-ESI/MS analysis. Food Chemistry 112 (1):226-231.

Lee, J.S., Kim, D.H., Liu, K.H., et al, 2005. Identification of flavonoids using liquid chromatography with electrospray ionization and ion trap tandem mass spectrometry with an MS/MS library. Rapid Commun. Mass Spectrom. 19 (23), 3539–3548.

Lei, F., Zhang, X., Wang, W., et al, 2007. Evidence of anti-obesity effects of the pomegranate leaf extract in high-fat diet induced obese mice. Int. J. Obesity 31 (6), 1023.

Lodhi, S., Jain, A.P., Sharma, V.K., et al, 2013. Wound-healing effect of flavonoid-rich fraction from *Tephrosia purpurea* Linn. on streptozotocin-induced diabetic rats. J. Herbs Spices Med Plants 19 (2), 191–205.

Ma, W., Guo, W., Shang, F. et al., 2020. Bakuchiol alleviates hyperglycemia-induced diabetic cardiomyopathy by reducing myocardial oxidative stress via activating the SIRT1/Nrf2 signaling pathway. Oxidative Medicine and Cellular Longevity 2020.

Martinez, R.M., Zarpelon, A.C., Zimermann, V.V., et al, 2012. *Tephrosia sinapou* extract reduces inflammatory leukocyte recruitment in mice: effect on oxidative stress, nitric oxide and cytokine production. Revista Brasileira de Farmacognosia 22 (3), 587–597.

Mosmann, T., 1983. Rapid Colorimetric Assay for Cellular Growth and Survival: Application to Proliferation and Cytotoxicity Assays. vol 65.

Natić, M.M., Dabić, D.Č., Papetti, A., et al, 2015. Analysis and characterisation of phytochemicals in mulberry (*Morus alba* L.) fruits grown in Vojvodina North Serbia. Food Chemistry 171, 128–136.

Nderitu, K.W., Mwenda, N.S., Macharia, N.J., et al, 2017. Antiobesity activities of methanolic extracts of *Amaranthus dubius, Cucurbita pepo,* and *Vigna unguiculata* in progesterone-induced obese Mice. Evidence-Based Complementary Alternative Medicine.

Ni, Y., Peng, Y., Kokot, S., 2008. Fingerprint analysis of Eucommia bark by LC-DAD and LC-MS with the aid of chemometrics. Chromatographia 67 (3–4), 211–217.

Nigam, R., Arnold, R., 2018. Phytochemical investigation and quantitative estimation of flavonoid and phenolic contents of the root, stem and leaves of *tephrosia purpurea* linn. Journal of Drug Delivery and Therapeutics 8 (5-s), 283–287.

Parmar, V., Jain, R., Gupta, S., et al, 1988. Phytochemical investigation of *Tephrosia candida*: HPLC separation of tephrosin and 12 α-hydroxyrotenone. J. Nat. Prod. 51 (1). 185-185.

Quifer-Rada, P., Vallverdú-Queralt, A., Martínez-Huélamo, M., et al, 2015. A comprehensive characterisation of beer polyphenols by high resolution mass spectrometry (LC–ESI-LTQ-Orbitrap-MS). Food Chem. 169, 336–343.

Roh, C., Jung, U., 2012. Screening of crude plant extracts with anti-obesity activity. Int. J. Mol. Sci. 13 (2), 1710–1719.

Roy, M., Mitra, S., Bhattacharyya, A., et al, 1986. Candidone, a flavanone from *Tephrosia candida*. Phytochemistry 25 (4), 961–962.

Sanz, M., de Simón, B.F., Cadahía, E., et al, 2012. LC-DAD/ESI-MS/MS study of phenolic compounds in ash (*Fraxinus excelsior* L. and F. *americana* L.) heartwood. Effect of toasting intensity at cooperage. J. Mass Spectrom. 47 (7), 905–918.

Seo, K.-H., Lee, D.-Y., Jeong, R.-H., et al, 2015. Neuroprotective effect of prenylated arylbenzofuran and flavonoids from morus alba fruits on glutamate-induced oxidative injury in HT22 hippocampal cells. J. Med. Food 18 (4), 403–408.

Shah, R., Parmar, S., Bhatt, P., et al, 2011. Evaluation of hepatoprotective activity of ethyl acetate fraction of *Tephrosia purpurea*. Pharmacologyonline 3, 188–194.

Sharaby, A., Ammar, N., 1997. Biological activity of extracts of Tephrosia nubica (Boiss) Baker against Spodoptera littoralis (Boisd.) and Agrotis ipsilon (Hufn.). Der Tropenlandwirt-J. Agriculture Tropics Subtropics 98 (2), 143–150.

Sharma, G.N., Gupta, G., Sharma, P., 2018. A comprehensive review of free radicals, antioxidants, and their relationship with human ailments. Crit. Rev. Eukaryot. Gene Expr. 28 (2), 139–154.

Simirgiotis, M.J., Benites, J., Areche, C., et al, 2015. Antioxidant capacities and analysis of phenolic compounds in three endemic Nolana species by HPLC-PDA-ESI-MS. Molecules 20 (6), 11490–11507.

Sindhu, G., Reddy, T., Kiran, U., et al, 2017. A review on the pharmacological profile of *Tephrosia calophylla*. Indo American Journal of Pharmaceutical Sciences 4 (5), 1361–1365.

Singh, S.P., Ali, M.M., Jain, G.K., 2010. High-throughput quantification of isoflavones, biochanin A and genistein, and their conjugates in female rat plasma using LC-ESI-MS/MS: Application in pharmacokinetic study. J. Sep. Sci. 33 (21), 3326–3334.

Solowey, E., Lichtenstein, M., Sallon, S. et al., 2014. Evaluating medicinal plants for anticancer activity. The Scientific World Journal 2014.

Spínola, V., Pinto, J., Castilho, P.C., 2015. Identification and quantification of phenolic compounds of selected fruits from Madeira Island by HPLC-DAD-ESI-MSn and screening for their antioxidant activity. Food Chem. 173, 14–30.

Srisawat, T., Chumkaew, P., Heed-Chim, W., et al, 2013. Phytochemical screening and cytotoxicity of crude extracts of *Vatica diospyroides* Symington Type LS. Trop. J. Pharm. Res. 12 (1), 71–76.

Stevens, J.F., Ivancic, M., Hsu, V.L., et al, 1997. Prenylflavonoids from *Humulus lupulus*. Phytochemistry 44 (8), 1575–1585.

Torre, L.A., Bray, F., Siegel, R.L. et al., 2015. Global cancer statistics, 2012. CA: A Cancer Journal for Clinicians 65 (2):87-108.

Touqeer, S., Saeed, M.A., Ajaib, M., 2013. A review on the phytochemistry and pharmacology of genus Tephrosia. Phytopharmacology 4 (3), 598–637.

Tripoli, E., La Guardia, M., Giammanco, S., et al, 2007. Citrus flavonoids: Molecular structure, biological activity and nutritional properties: A review. Food Chem. 104 (2), 466–479.

Vladimir-Knežević, S., Blažeković, B., Bival Štefan, M., et al, 2011. Antioxidant activities and polyphenolic contents of three selected *Micromeria* species from Croatia. Molecules 16 (2), 1454–1470.

Wannes, W.A., Tounsi, M.S., Marzouk, B., 2017. A review of Tunisian medicinal plants with anticancer activity. J. Complementary Integrative Medicine 15 (1).

Winarsi, H., Yuniaty, A., 2019. Antioxidant exploration in cardamom rhizome potential as a functional food ingredient. IOP Conference Series: Earth and Environ. Sci. 1, 012019.

Xu, M.J., Wu, B., Ding, T., et al, 2012. Simultaneous characterization of prenylated flavonoids and isoflavonoids in *Psoralea corylifolia* L. by liquid chromatography with diode-array detection and quadrupole time-of-flight mass spectrometry. Rapid Commun. Mass Spectrom. 26 (19), 2343–2358.

Yajima, H., Noguchi, T., Ikeshima, E., et al, 2005. Prevention of diet-induced obesity by dietary isomerized hop extract containing isohumulones, in rodents. Int. J. Obesity 29 (8), 991.

Ye, J.-B., Ren, G., Li, W.-Y., et al, 2019. Characterization and identification of prenylated flavonoids from *Artocarpus heterophyllus* Lam. roots by Quadrupole Time-of-Flight and Linear Trap Quadrupole Orbitrap Mass spectrometry. Molecules 24 (24), 4591.

Yen, G.C., Duh, P.D., 1994. Scavenging effect of methanolic extracts of *peanut hulls* on free-radical and active-oxygen species. J. Agric. Food Chem. 42 (3), 629–632.

Zemmouri, H., Ammar, S., Boumendjel, A. et al., 2014. Chemical composition and antioxidant activity of Borago officinalis L. leaf extract growing in Algeria. Arabian Journal of Chemistry 12 (8):1954-1963.

Zhang, X., Zhao, W., Wang, Y., et al, 2016. The chemical constituents and bioactivities of *Psoralea corylifolia* Linn.: a review. Am. J. Chinese Med. 44 (01), 35–60.

Ziani, B.E., Barros, L., Boumehira, A.Z., et al, 2018. Profiling polyphenol composition by HPLC-DAD-ESI/MSn and the antibacterial activity of infusion preparations obtained from four medicinal plants. Food Funct. 9 (1), 149–159.

Zielinska-Blizniewska, H., Sitarek, P., Merecz-Sadowska, A., et al, 2019. Plant extracts and reactive oxygen species as two counteracting agents with anti-and pro-obesity properties. Int. J. Mol. Sci. 20 (18), 4556.